

## Shear Strength of Steel Beams with Trapezoidal Corrugated Webs Using Regression Analysis

Samer Barakat<sup>1</sup>, Ahmad Al Mansouri<sup>2</sup>, Salah Altoubat<sup>3</sup>

*Department of Civil and Environmental Engineering  
University of Sharjah, Sharjah, UAE*

<sup>1</sup> e-mail: [sbarakat@sharjah.ac.ae](mailto:sbarakat@sharjah.ac.ae), web page: <http://www.sharjah.ac.ae/>

<sup>2</sup> e-mail: [ahmadalmansouri@gmail.com](mailto:ahmadalmansouri@gmail.com)

<sup>3</sup> e-mail: [saltoubat@sharjah.ac.ae](mailto:saltoubat@sharjah.ac.ae), web page: <http://www.sharjah.ac.ae/>

**Keywords :** Shear strength, Steel Beams, Trapezoidal Corrugated Web, Regression

### Abstract

It was recognized from theoretical and experimental results that the shear buckling strength of a steel beam with corrugated web is complicated and affected by several parameters. A model that predicts the shear strength of a steel beam with corrugated web with reasonable accuracy was sought. To that end, multiple regression analysis (MRA) with a total of 93 collected experimental data points were used for modeling and predicting the shear buckling strength of a steel beam with corrugated web. Then mathematical models for the key response parameter (shear buckling strength of a steel beam with corrugated web) were established via MRA in terms of different input geometric, loading and materials parameters. MRA model having an  $R^2$  value of 0.93 and passing the F- and t-tests were selected. Results indicate that, MRA could accurately predict the shear buckling strength of a steel beam with corrugated web with a minimal processing of data.

---

## 1. Introduction

Steel beams with corrugated webs are a relatively recent development in structural systems and have seen a lot of use in bridge construction. They are typically composed of corrugated steel plates (forming the web) that are welded to a pair of flanges. The corrugations can take many shapes: rectangular, triangular, semi-circular, sinusoidal, and trapezoidal (Fig. 1), the latter of which is the focus of this paper. Fig.1a shows an example of a trapezoidal corrugated steel beam. Fig.1b shows a cross-section through that beam and identifies all the relevant geometric properties for such a configuration: the length of the horizontal corrugation ( $a$ ), the length of the horizontal projection of the diagonal corrugation ( $b$ ), the length of the diagonal corrugation ( $c$ ), the depth of the corrugation ( $d$ ), the angle of corrugation ( $\theta$ ), and the thickness of the web ( $t_w$ ).

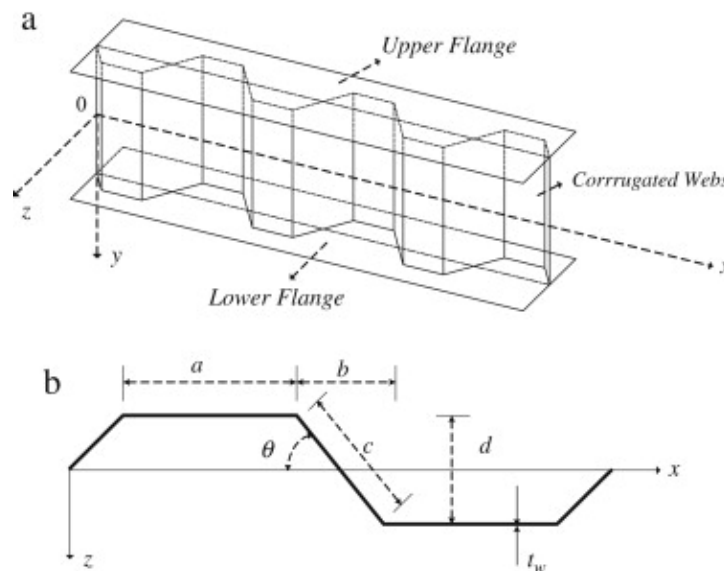


Fig. 1. I-girder with corrugated steel webs: (a) Profile; (b) Geometric notations (Moon et. al 2009).

Steel beams with corrugated webs have higher shear strength than beams with straight webs alleviating the need for transverse stiffeners. A number of theoretical and experimental studies have been carried out to quantify the increase in shear strength of the section in terms of the geometry of the corrugations and the material properties (see for example Abbas et. al. (2002) and (2006), Gil et. al (2005), Yi et. al (2008), Sause and Braxtan (2011), and El Metwally (1998). All in all, Sause and Braxtan collected a total of 102 data points. However, because El Metwally's equation was derived from the local and global buckling theories, Sause and Braxtan could only use 22 of the 102 results in their study, as those were the only results originating from test conditions that were compatible with the assumptions of the theories. The motivation behind this paper is to find a more inclusive equation to calculate the shear buckling strength of beams with corrugated webs that would not be subject to the same restrictions. To that end, the approach of this paper will be to derive an equation from the test results themselves, setting aside a portion of the results to verify the accuracy of the equation. It should be noted that this paper will refer to the dimensions of the corrugated web using the notation defined in Sause and Braxtan (2011), which is shown in Fig. 2. It should also be noted that this notation is different to that of Fig. 1.

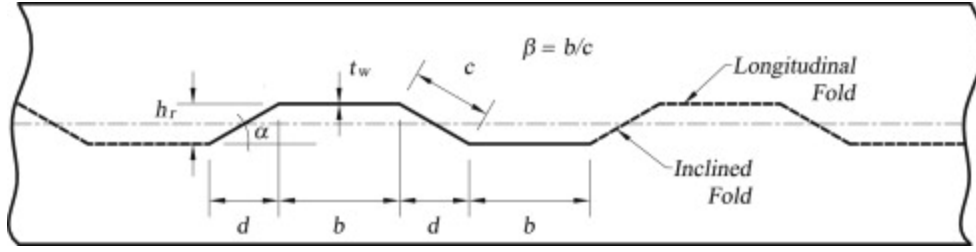


Fig. 2. Beam with corrugated web (section through web), Sause and Braxtan (2011).

Two modes of shear buckling are defined: local and global buckling. Local buckling refers to deformations occurring in individual folds of the web. These deformations can occur simultaneously in multiple folds and can propagate into adjacent unaffected folds. Global buckling, on the other hand, occurs over several folds, the buckled shape extending diagonally over the depth of the web. Because of the similarity between global buckling and multiple simultaneous local buckling, experimentally observed buckling often appears to have characteristics of both modes. The local elastic shear buckling stress,  $\tau_{L,el}$ , can then be expressed as:

$$\tau_{L,el} = k_L \frac{\pi^2 E}{12(1-\nu^2)(w/t_w)^2} \quad (1)$$

where  $k_L$  is a coefficient that depends on the aspect ratio of the folds and the boundary conditions of the beam,  $E$  is Young's modulus,  $\nu$  is Poisson's ratio,  $w$  is the fold width, and  $t_w$  is the thickness of the web. Of these values, only  $w$ , the fold width, changes from fold to fold. For longitudinal folds,  $w = b$  (Fig. 2), and for inclined folds,  $w = c$ . The larger of  $b$  and  $c$  is taken to determine the smallest value of  $\tau_{L,el}$ .

Similarly, an expression for the global shear buckling stress for a corrugated plate can be derived from the orthotropic plate theory. Easley (1975) developed the following expression for the global shear buckling stress  $\tau_{G,el}$ :

$$\tau_{G,el} = k_G \frac{(D_y)^{1/4} \cdot (D_x)^{3/4}}{t_w \cdot h_w^2} \quad (2)$$

where  $k_G$  is a coefficient that depends on the boundary conditions of the plate.  $D_y$  and  $D_x$  are defined as follows:

$$D_y = \frac{b+d}{b+d \cdot \sec(\alpha)} \cdot \frac{E \cdot t_w^3}{12} \quad (3)$$

$$D_x = \frac{E}{b+d} \left( \frac{b \cdot t_w \cdot (d \cdot \tan(\alpha))^2}{4} + \frac{t_w \cdot (d \cdot \tan(\alpha))^3}{12 \sin(\alpha)} \right) \quad (4)$$

where  $\alpha$  is the angle of corrugation and  $d$  is the longitudinal projection of the inclined fold, as shown in Fig. 2.

In his Ph.D. dissertation, Abbas combined Equations (2)-(4) to express the global shear buckling stress directly in terms of the geometric parameters shown in Fig. 2:

$$\tau_{G,el} = k_G F(\alpha, \beta) \frac{E t_w^{1/2} b^{3/2}}{12 h_w^2} = C_G \frac{E t_w^{1/2} b^{3/2}}{12 h_w^2} \quad (5)$$

where  $F(\alpha, \beta)$  is a coefficient based on the dimensions of the corrugations of the web, defined as follows:

$$F(\alpha, \beta) = \sqrt{\frac{1 + \beta \sin^3 \alpha}{\beta + \cos \alpha}} \cdot \left\{ \frac{3\beta + 1}{\beta^2(\beta + 1)} \right\}^{3/4} \quad (6)$$

where  $\beta$  is the ratio of  $b$  to  $c$ . It is possible that an interaction between local and global buckling modes exist. Past studies have attempted to illustrate this relationship and demonstrate its effect on both buckling modes using interaction formulas. One such formula, proposed by Linder and Aschinger (1998), can be expressed as follows:

$$\frac{1}{(\tau_{I,el})^n} = \frac{1}{(\tau_{L,el})^n} + \frac{1}{(\tau_{G,el})^n} \quad (7)$$

where  $\tau_{I,el}$  is the elastic shear buckling stress due to interaction and  $n$  is an integer. Yi et al. [8] proposed a formula based on Equation (7) with  $n = 1$ . Solving for  $\tau_{I,el}$ , that formula becomes:

$$\tau_{I,n,el} = \frac{\tau_{L,el} \cdot \tau_{G,el}}{((\tau_{L,el})^n + (\tau_{G,el})^n)^{1/n}} \quad (8)$$

The local, global and interaction buckling slenderness ratios are defined as follows, respectively:

$$\lambda_L = \sqrt{\frac{\tau_y}{\tau_{L,el}}} = \sqrt{\frac{12(1-\nu^2)\tau_y w}{k_L \pi^2 E t_w}} \quad (9)$$

$$\lambda_G = \sqrt{\frac{\tau_y}{\tau_{G,el}}} = \sqrt{\frac{12\tau_y \cdot h_w^2}{k_G \cdot F(\alpha, \beta) \cdot E \cdot t_w^{1/2} \cdot b^{3/2}}} \quad (10)$$

$$\lambda_{I,n} = \sqrt{\frac{\tau_y}{\tau_{I,n,el}}} = \lambda_L \lambda_G ((1/\lambda_L)^{2n} + (1/\lambda_G)^{2n})^{1/2n} \quad (11)$$

where the exponent  $n$  is an integer and  $\tau_y$  is the shear yield stress according to the Von Mises yield criterion, defined as:

$$\tau_y = \frac{F_y}{\sqrt{3}} \quad (12)$$

and  $F_y$  is the uniaxial yield stress of the web.

The normalized local, global, and interaction elastic shear buckling strengths can be determined from the slenderness ratios. They are, respectively:

$$\rho_{L,el} = \frac{1}{\lambda_L^2} \quad (13)$$

$$\rho_{G,el} = \frac{1}{\lambda_G^2} \quad (14)$$

$$\rho_{I,n,el} = \frac{1}{\lambda_{I,n}^2} \quad (15)$$

It should be noted that all of the equations thus far have only considered elastic shear buckling stress.

## 2. Multiple Regression Analysis (MRA)

### 2.1 Linear Regression Models

Out of the 102 data points, 8 are omitted because their shear span,  $a$ , was not reported. Each of the 93 remaining data points is randomly assigned to one of two sets. 73 data points are assigned to set 1, from which the linear regression model is to be derived. 20 data points are assigned to set 2, against which the results of the linear regression model are to be checked. The linear regression model between the dependent variable ( $\rho_e$ ) and the all independent variables ( $h_w$ ,  $t_w$ ,  $a$ ,  $b$ ,  $c$ ,  $\alpha$ ,  $F_y$ ) is then calculated using data set 1. Table 1 summarizes the SPSS outputs for the  $\rho_e$  model. Despite the apparent good-fitting and passing the F-test, the linear model is deemed physically unsound for the  $\rho_e$  prediction. This is attributed to the negative signs on two of the independent variables coefficients, and the negligibly small coefficients of two others. For example, this implies that increasing the shear span ( $a$ ) or the length of the diagonal fold ( $c$ ) decreases  $\rho_e$ , and that changing the yield stress ( $F_y$ ) doesn't change  $\rho_e$ , which is counterintuitive. Moreover, two coefficients (those of  $a$  and  $c$ ) fail the t-test. Consequently, nonlinear regression models are reverted to.

Table 1: Linear regression results

$R^2$	F-value		F-significance
0.965	258.882		0
Variable	Coefficient	t-value	t-significance
$h_w$	0.000	2.087	0.41
$a$	-2.087E-005	-0.412	0.682
$t_w$	0.105	5.042	0.000
$b$	0.002	1.764	0.082
$\alpha$	0.009	4.304	0.000
$c$	-0.003	-2.393	0.020
$F_y$	0.000	1.310	0.195

## 2.2 Nonlinear Regression Models

Nonlinear regression is appropriate when the relationship between the dependent and independent variables is not intrinsically linear. Therefore, new nonlinear functions are created from the original variables in the original data set. These new variables are created in forms that guarantee that the curved functions of the original variables are transformed to linear functions of the new variables. Based on several trials of functions that preserve the physical interpretation, many transformation functions were obtained. Noting the aforementioned relationship between the slenderness ratios and the theoretical normalized shear buckling strengths (see Eqs. 13-15), it was proposed that there could similarly be good correlation between the slenderness ratios and the shear buckling strength derived from the experimental results. In order to investigate this potential relationship the experimental normalized shear buckling strength  $\rho_e$  was plotted against each of the slenderness ratios (Fig. 3). The distribution of data points in Fig. 3 indicates a significant inversely proportional relationship between  $\rho_e$  and  $\lambda_{l,1}$  (Eq. (11) with  $n = 1$ ).

Performing linear regression between  $\rho_e$  and  $1/\lambda_{l,1}$  confirms this relationship, producing an  $R^2$  value of 0.934, as well as passing the F- and t-tests (see Table 2).

Therefore, the best discovered regression model is as follows:

$$\rho_e = 0.747/\lambda_{l,1} \quad (16)$$

Where

$$\lambda_{l,1} = \lambda_L \lambda_G \sqrt{((1/\lambda_L)^2 + (1/\lambda_G)^2)} \quad (17)$$

and  $\lambda_L$  and  $\lambda_G$  are as in Equations (9) and (10), respectively.

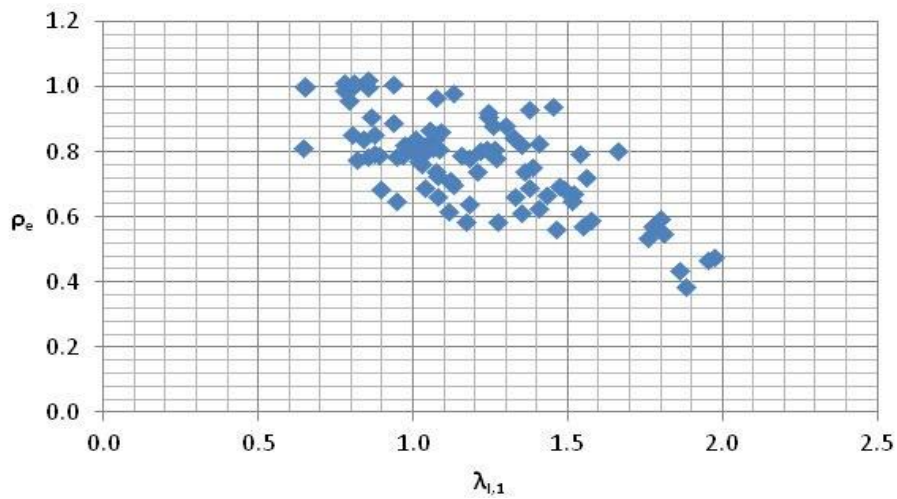
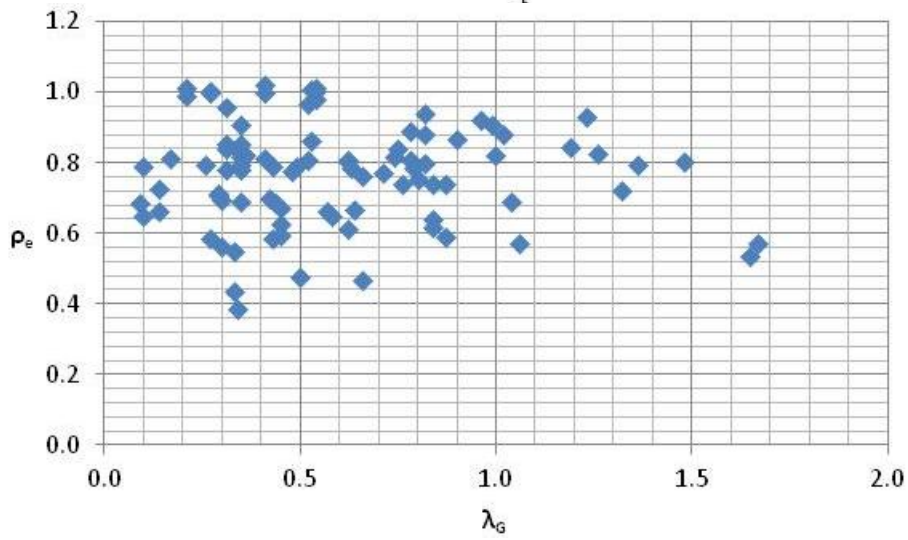
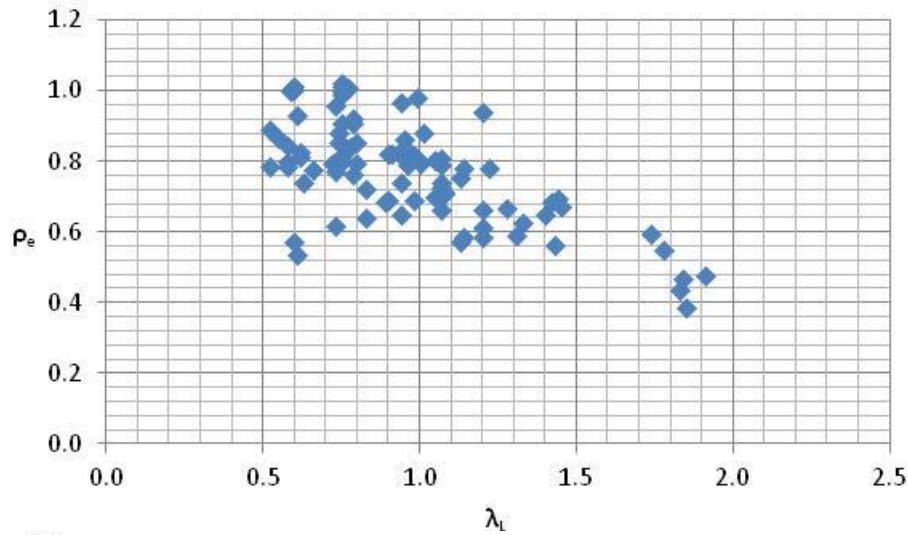


Fig. 3: Normalized shear buckling strength  $\rho_e$  vs. a) local slenderness ratio  $\lambda_L$ , b) global slenderness ratio  $\lambda_G$ , c) interactive slenderness ratio  $\lambda_I$

Table 2: Nonlinear regression results

$R^2$	F-value	F-significance	
0.930	956.704	0	
Variable	Coefficient	t-value	t-significance
$1/\lambda_{I,1}$	0.747	30.931	0

The accuracy of the regression models was checked. The input values from set 1 of data were presented to the MRA model to perform the necessary calculations and produce the corresponding outputs. Comparison of experimental values and predicted values of the shear buckling strength of a steel beam with corrugated web by MRA are presented in Fig. 4.

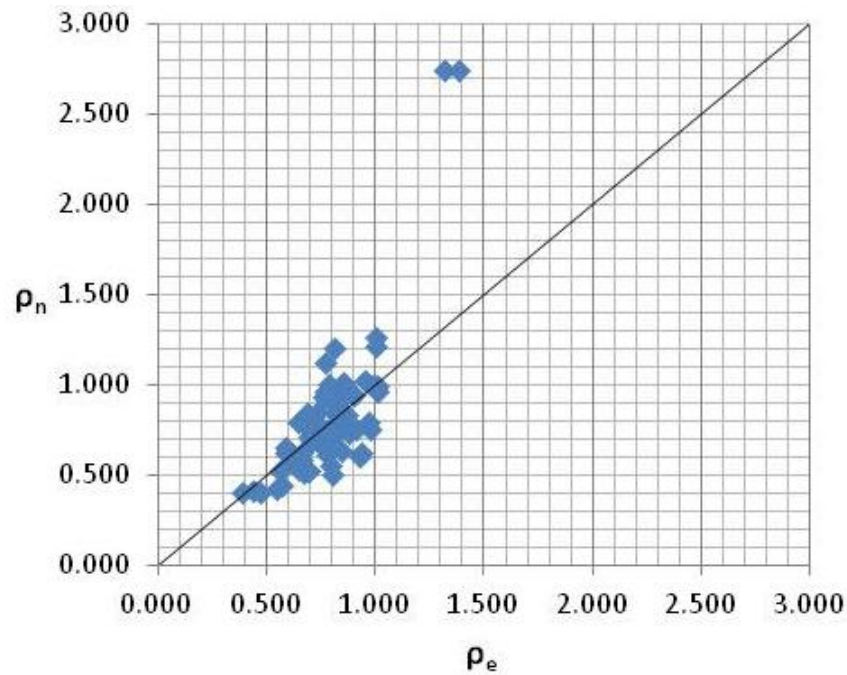


Fig. 4: Set 1's recalled normalized shear buckling strength  $\rho_n$  vs. experimental  $\rho_e$

Furthermore, the prediction accuracy of the model adopted in this work was also checked. One additional set 2 of data consisting of 20 points were used to perform the prediction test using the MRA model. It should be stressed that all of the data in this later set was initially withheld from the MRA. The results of this test are shown in Fig. 5. The closeness of the points to the equality line serves only to indicate the validity of the MRA model.

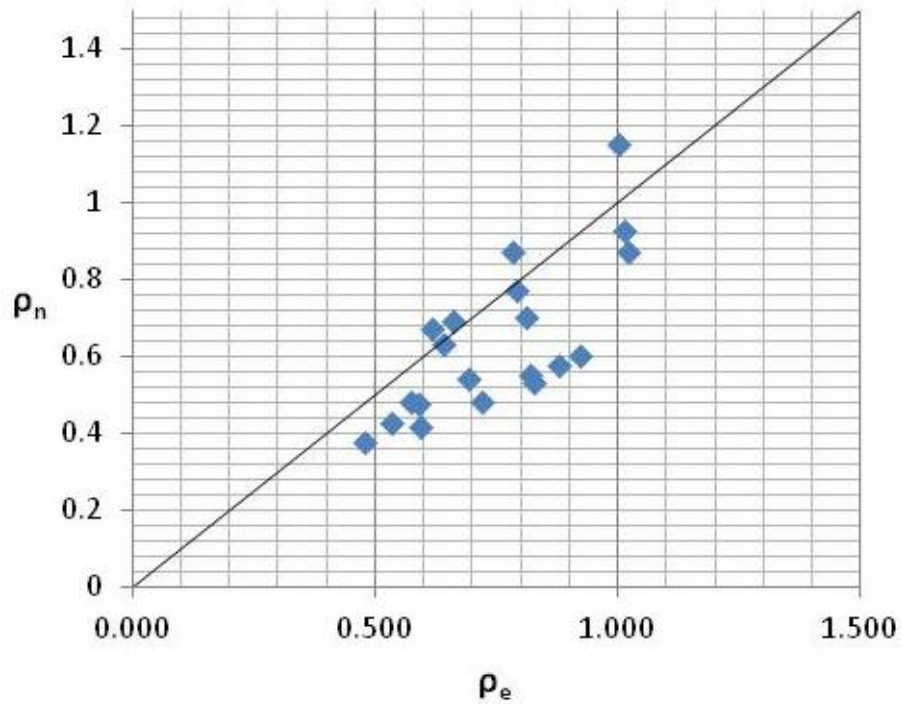


Fig.5: Set 2's predicted normalized shear buckling strength  $\rho_n$  vs. experimental  $\rho_e$

### 3. Summary and Conclusions

A multiple linear regression model was developed for predicting the shear buckling strength of corrugated web steel sections based on the observed relationship between the interactive slenderness ratios of some sections and their normalized experimental shear buckling strength. A number of different models were tested before settling on one that produced satisfactory results. The final model had an  $R^2$  value of 0.93 and passed the F- and t-tests. With this model, it is possible to predict the shear buckling strength of corrugated web sections from their geometric and material properties with good accuracy.



## References

- Abbas HH, Sause R, Driver RG (2006). "Behavior of corrugated web I-girders under in-plane loading," J Struct Eng, ASCE; **132(8)**:806-14.
- El Metwally A. S. (1998), *Prestressed composite girders with corrugated steel webs*, Calgary: University of Calgary.
- Elgaaly M., Hamilton R. W. and Seshadri A. (1996), "Shear Strength of Beams with Corrugated Webs," Journal of Structural Engineering, **vol. 122, no. 4**, 390-398.
- Easley J. T. (1975), "Buckling formulas for corrugated metal shear diaphragms," Journal of the Structural Division, **vol. 101, no. 7**, 1403-1417.
- Gil H, Lee S, Lee J, Lee HE (2005). "Shear buckling strength of trapezoidally corrugated steel webs for bridges." J Transport Res Board; CD11-S:473-480.
- Moon J., Yi J., Choi B. H. and Lee H.-E. (2009), "Shear strength and design of trapezoidally corrugated steel webs," Journal of Constructional Steel Research, **vol. 65, no. 5**, 1198–1205.
- Sause R. and Braxtan T. N. (2011), "Shear strength of trapezoidal corrugated steel webs," Journal of Constructional Steel Research, **vol. 67, no. 2**, 223-236.
- Timoshenko S. P. and Gere J. M. (2009), *Theory of Elastic Stability* (Dover Civil and Mechanical Engineering), New York: Dover Publications.
- Yi J., Gil H., Youm K. and Lee H. (2008), "Interactive shear buckling behavior of trapezoidally corrugated steel webs," Engineering Structures, **vol. 30, no. 6**, 1659–1666.